

# Molecular Dynamics Simulations of the Initial-State Predict Product Distributions of Dediazonation of Aryldiazonium in Binary Solvents

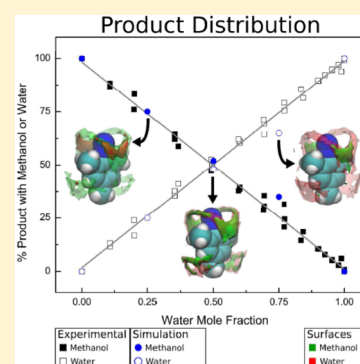
Gustavo N. Cruz,<sup>†</sup> Filipe S. Lima,<sup>\*,†</sup> Luís G. Dias,<sup>‡</sup> Omar A. El Seoud,<sup>§</sup> Dominik Horinek,<sup>||</sup> Hernan Chaimovich,<sup>†</sup> and Iolanda M. Cuccovia<sup>\*,†</sup>

<sup>†</sup>Departamento de Bioquímica, <sup>§</sup>Instituto de Química, and <sup>‡</sup>Department of Química, Fac. Filosofia, Ciências e Letras de Ribeirão Preto, Universidade de São Paulo, São Paulo, Brazil

<sup>||</sup>Institute für Physikalische und Theoretischen Chemie, University of Regensburg, 93053 Regensburg, Germany

**S** Supporting Information

**ABSTRACT:** The dediazonation of aryldiazonium salts in mixed solvents proceeds by a borderline  $S_N1$  and  $S_N2$  pathway, and product distribution should be proportional to the composition of the solvation shell of the carbon attached to the  $-N_2$  group (ipso carbon). The rates of dediazonation of 2,4,6-trimethylbenzenediazonium in water, methanol, ethanol, propanol, and acetonitrile were similar, but measured product distributions were noticeably dependent on the nature of the water/cosolvent mixture. Here we demonstrated that solvent distribution in the first solvation shell of the ipso carbon, calculated from classical molecular dynamics simulations, is equal to the measured product distribution. Furthermore, we showed that regardless of the charge distribution of the initial state, i.e., whether the positive charge is smeared over the molecule or localized on phenyl moiety, the solvent distribution around the reaction center is nearly the same.



## INTRODUCTION

The capacity of some probes to distinguish different media has been used to investigate micelles, membranes, cell compartments, enzyme active sites, etc.<sup>1</sup> Diazonium salts have been used to determinate the concentration of anions at the surface of micelles, liposomes, and reverse micelles.<sup>2</sup> The low sensitivity of the diazonium salts reaction rates to solvent polarity and the reaction of the intermediate carbocation with different nucleophiles, following first-order kinetics,<sup>3</sup> has been used as a good argument for using these probes as a tool for the determination of anions concentration in several condensed media.<sup>2</sup>

On the basis of extensive experimental evidence, a  $S_N1$  mechanism, with the intermediate formation of a very reactive phenyl cation, was thought to be the only reaction pathway.<sup>3</sup> Alternative mechanisms, assuming specific water and nucleophile interactions in the initial state, have been presented, and the nucleophilic displacement process for aryldiazonium ions in water is proposed to be at the boundary between  $S_N2$  and  $S_N1$ .<sup>4–6</sup> Recently, excellent agreement was found between in-water theoretical activation free energies calculated according to the Marcus theory with the corresponding experimental data when assuming the  $S_N2$  rather than  $S_N1$  mechanisms.<sup>7</sup>

For solvent mixtures, as in the solvolysis of 4-methylbenzenediazonium ions in 2,2,2-trifluoroethanol–water, the kinetic and thermodynamic results suggest that the rate-determining step for dediazonation is the formation of a highly reactive aryl cation that traps any nucleophile available in its solvation shell.<sup>8</sup> The major products of the dediazonation of 2-, 3-, and 4-

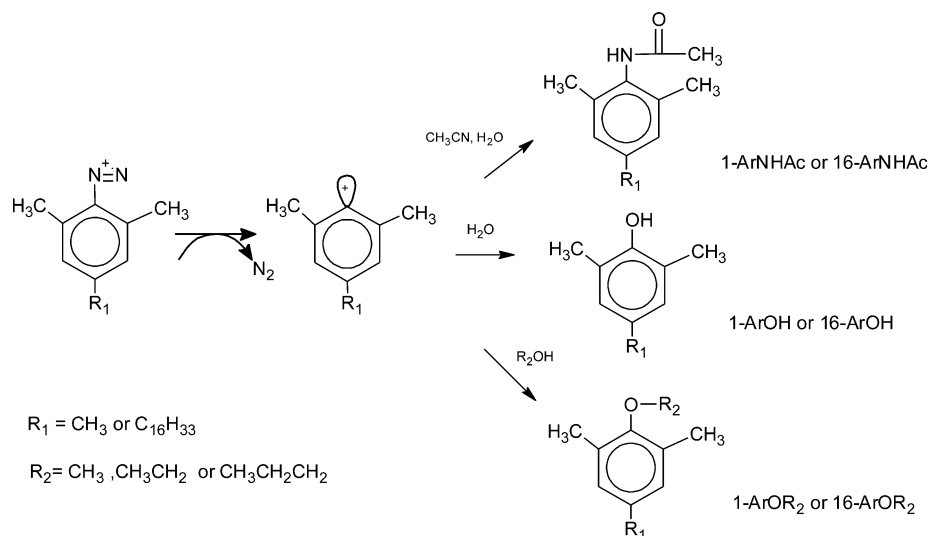
methylbenzenediazonium ions in ethanol/water mixtures are ethyl methylphenyl ethers and cresols.<sup>9</sup> All three compounds produce equal amounts of products in a water molar fraction ( $x_{\text{water}} = n_{\text{water}}/(n_{\text{water}} + n_{\text{solvent}})$ ) equal to 0.36. The authors suggest that the observed product distribution reflects the nucleophile distribution in the first solvation shells of the arenediazonium ions. An underlying simplification is the assumption that, in the case of an  $S_N1$  reaction mechanism, the reaction is fast and the reorganization of the solvent when the intermediate is formed is neglected. In butanol and water mixtures, *o*-methyldiazonium decomposes producing *o*-methylphenol and 1-butoxy-2-methylbenzene. In this reaction 50% of each product is obtained at  $x_{\text{water}} = 0.34$ , suggesting that the diazonium ion undergoes preferential solvation by water.

Here, we examined the rate and products of the dediazonation of 2,4,6-trimethylbenzenediazonium ion in mixtures of water/acetonitrile and water/alcohols: water/methanol, water/ethanol, and water/propanol (Scheme 1, for sake of brevity,  $S_N1$  mechanism is presented). In addition, we have carried out classical molecular dynamics (MD) simulations (i.e., no bond breaking/forming in the simulations) of solvent distribution around  $1\text{-ArN}_2^+$  for water/solvent mixtures showing that the preferential solvation around ipso carbon reflects the experimental product yields of dediazonation. Such theoretical evidence should be valid when nucleophilic reactivities are similar and reactions occur at the

Received: June 8, 2015

Published: August 11, 2015

Scheme 1



$S_N1$  (or  $S_N1/S_N2$  borderline) mechanism.<sup>6,10</sup> Such a simple protocol is a shortcut for the more extensive reactive trajectories calculations at the femtosecond time scale.<sup>6,11–13</sup> Interestingly, preferential solvation was only marginally dependent on ipso carbon charge distribution.

## RESULTS

### The Decomposition of 1- $\text{ArN}_2^+$ in Solvent Mixtures.

**Product Yields in Methanol.** The rate constant for the solvolysis of 1- $\text{ArN}_2^+$  in water and methanol (30 °C) were  $8.2 \times 10^{-3}$  and  $9.9 \times 10^{-3} \text{ min}^{-1}$  ( $\pm 5\%$ ), respectively. The main reaction products were 2,4,6-trimethylphenol (1- $\text{ArOH}$ ) and 2,4,6-trimethylanisole (1- $\text{ArOMe}$ ). A small percentage ( $<0.5\%$ ) of 2,4,6-trimethylbenzene (1- $\text{ArH}$ ), the reduced product of 1- $\text{ArN}_2^+$ , and traces of 2,4,6-trimethyl chloride (1- $\text{ArCl}$ ), due the presence of ca.  $10^{-3} \text{ mol dm}^{-3}$  HCl, were formed, consistent with other studies reported with similar diazonium salts.<sup>14</sup>

The increase in water mole fraction [(water moles)/(water moles + MeOH moles)] in water/methanol mixtures produced a linear increase of the 1- $\text{ArOH}$  molar concentration and an equivalent decrease in the molar concentration of 1- $\text{ArOMe}$  (Figure 1). In Figure 1, the amount of products formed is given in percentage (%) of the total diazonium salt [1- $\text{ArN}_2^+$ ]<sub>T</sub>. As only traces of 1- $\text{ArH}$  and 1- $\text{ArCl}$  were formed in all water/methanol mixtures, their concentrations were subtracted from the total concentration of 1- $\text{ArN}_2^+$ . Thus, the sum of [1- $\text{ArOH}$ ] and [1- $\text{ArOMe}$ ] was equal to [1- $\text{ArN}_2^+$ ]<sub>T</sub>:

$$[1-\text{ArN}_2^+]_{\text{T}} = [1-\text{ArOH}] + [1-\text{ArOMe}] \quad (1)$$

The %1- $\text{ArOH}$  linearly increased and that of %1- $\text{ArOMe}$  linearly decreased with the water mole fraction. With a water mole fraction of 0.5, the percentages of 1- $\text{ArOH}$  and 1- $\text{ArOMe}$  were identical (i.e., 50%) (see Figure 1).

**Product Yields in Ethanol and Propanol.** The solvolysis of 1- $\text{ArN}_2^+$  was also studied in mixtures of water/ethanol and water/*n*-propanol where 1- $\text{ArOH}$  and the ethers 1- $\text{ArOEt}$  and 1- $\text{ArOPr}$  were formed, respectively. The rate constants of 1- $\text{ArN}_2^+$  dediazonation with ethanol and propanol were  $8.2 \times 10^{-3}$  and  $7.1 \times 10^{-3} \text{ min}^{-1}$  ( $\pm 5\%$ ), respectively.

Figure 2 shows the % products formed in those mixtures, and different from the results obtained with water/methanol mixtures, the plots of % products vs water mole fraction in

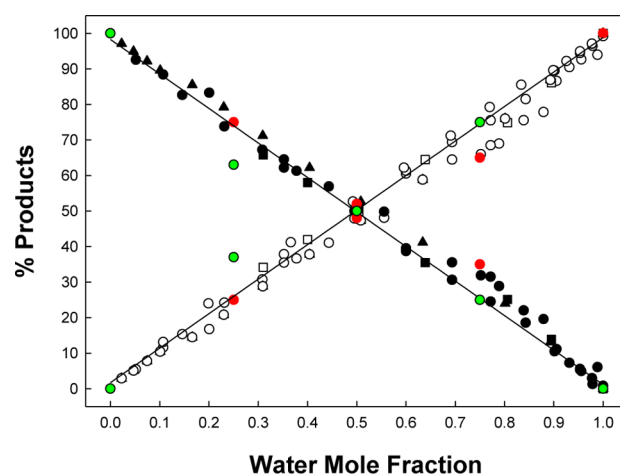


**Figure 1.** Effect of water mole fraction in the % Products of 1- $\text{ArN}_2^+$  and 16- $\text{ArN}_2^+$  reactions in Methanol/Water: 1- $\text{ArOH}$  (○,□); 1- $\text{ArOMe}$  (●,■) (Two sets of experiments); 16- $\text{ArOH}$  (△); 16- $\text{ArOMe}$  (▲). MD simulations, (red solid circle) M1 model, and (green solid circle) M2 model. Black lines are linear fits to % 1- $\text{ArX}$ .

both solvent mixtures were not linear. The formation of 50% of each product occurred at 0.36 and 0.32 water mole ratio for water/ethanol and water/*n*-propanol, respectively (Figure 2). As the chain of the alcohol increased from ethanol to propanol, 50% of each product occurred at even lower water mole ratios. The effect was observed previously with water/butanol mixtures by Bravo and co-workers in monosubstituted methyl-benzenediazonium salts.<sup>15</sup>

**Product Yields in Acetonitrile.** The rate constant of 1- $\text{ArN}_2^+$  with acetonitrile was  $10.1 \times 10^{-3} \text{ min}^{-1}$  ( $\pm 5\%$ ). In water/acetonitrile mixtures, 1- $\text{ArN}_2^+$  reacts with acetonitrile producing the acetamides (1- $\text{ArNHAc}$ ).<sup>17</sup> 1- $\text{ArH}$  was not formed in a significant amount in those mixtures. The %1- $\text{ArOH}$  and %1- $\text{ArNHAc}$  were nonlinearly related to the water mole fraction (Figure 3), and 50% of each product was formed when water/acetonitrile molar fraction was about 0.7.

**Molecular Dynamics Simulations.** The  $\theta_Z$  is the theoretical fraction (in percentage) of a given nucleophile relative to the total nucleophiles in the first solvation shell of the ipso carbon. Simulations were carried out with a charge model (M1)

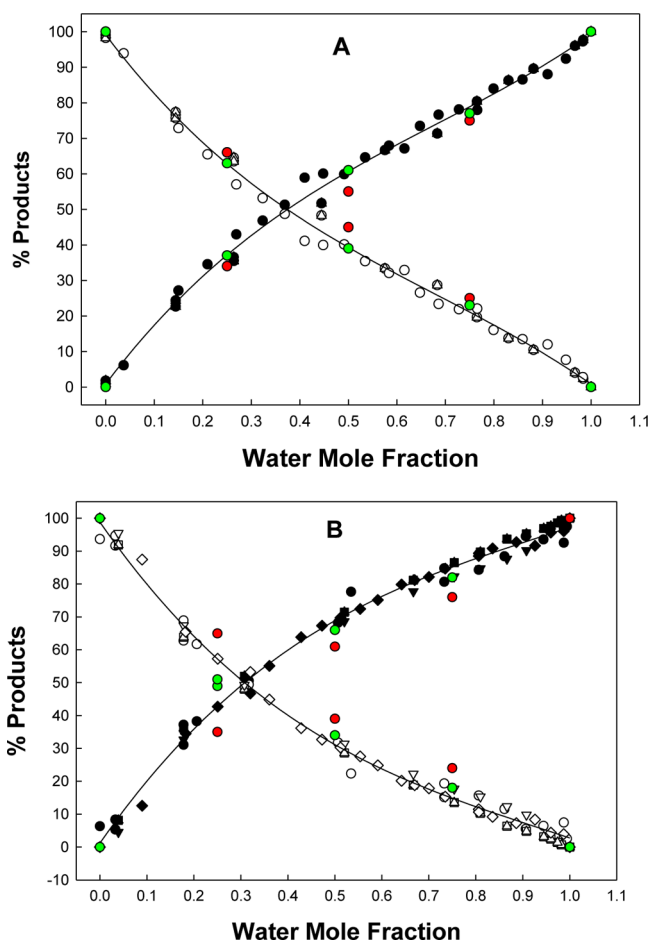


**Figure 2.** Effect of water mole fraction in the % products of 1-ArN<sub>2</sub><sup>+</sup> and 16-ArN<sub>2</sub><sup>+</sup> reactions in solvent mixtures. MD simulations, (red solid circle) M1 model and (green solid circle) M2 model. (A) Ethanol/water: 1-ArOH (○, □); 1-ArOEt (●, ■). Solid black lines are third-order polynomials adjust to % 1-ArX. (B) Propanol/water: Different symbols for the same product are related to independent sets of experiments: 1-ArOH (○, □, △, ◇); 1-ArOPr (●, ▲, ■, ◆); 16-ArOH (▽), 16-ArOPr (▼).

modeling the rupture of ipso carbon and nitrogen bond. Simulations were also carried using a charge model based on a stable 1-ArN<sub>2</sub><sup>+</sup> cation (the M2 model). Such charge models gave different atomic charges at ipso carbon (M1: +0.61|e|; M2: -0.46|e|). However, the composition of the solvation shell around the ipso carbon was only slightly dependent on the M1 and M2 charge models. An additional rule must be provided to link the solvation shell composition with products percentage (% product). The assumption was that nucleophiles have equal probabilities to react on ipso carbon site (in low selectivity case). Therefore, comparisons between  $\theta_z$  and % products (in measurements described above) were straightforward and presented in Figures 1, 2, and 3. For the four binary mixtures studied here, the  $\theta_z$  values of the organic solvents decreased as the  $x_{\text{water}}$  increased. In methanol/water mixture, both  $\theta_z$  and % products showed a nearly linear behavior, and the water fraction at which  $\theta_{\text{water}} = 50$  ( $x_{1/2}$ ) was equal to 0.5. However, a nonlinear dependence of  $\theta_z$  with  $x_{\text{water}}$  was found for the other solvent mixtures, as can be seen in Figures 1 and 2. The MD results showed a good agreement with experimental values, regardless of the nature of the organic solvent and the charge distribution model used for the probe. As experimentally

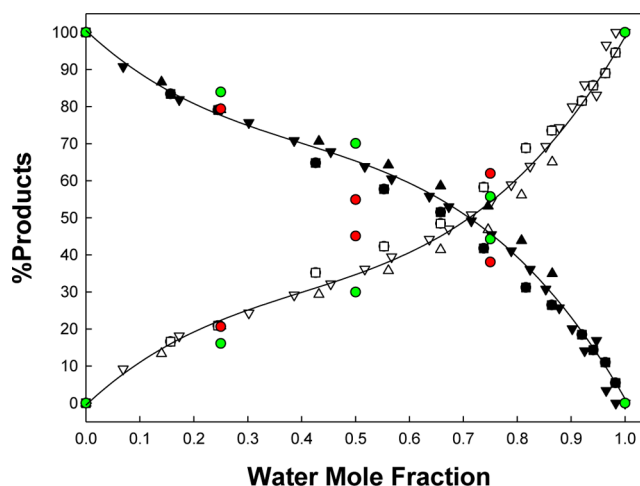


**Figure 3.** Effect of water mole fraction in the % products of 1-ArN<sub>2</sub><sup>+</sup> and 16-ArN<sub>2</sub><sup>+</sup> in Acetonitrile/Water. Different symbols for the same product are related to independent sets of experiments: 1-ArOH (△, ▽); 1-ArNHCN (▲, ▼) (Two sets of different experiments), 16-ArOH (□); 16-ArNHAc (■); (red solid circle) M1 model and (green solid circle) M2 model. Solid black lines are third-order polynomials adjust to % 1-ArX.

observed, the  $x_{1/2}$  values decreased in the order acetonitrile > methanol > ethanol > propanol.

## DISCUSSION

The low sensitivity of dediazonation reactions can be related to the nucleophilic scales. Ritchie used substituted aryldiazonium cations in his  $N_+$  ( $\equiv \log(k/k_{\text{H}_2\text{O}})$ ) scale.<sup>16,17</sup> Using our kinetic data for pure solvents and water,  $N_+$  (in this case, cation dependent) resulted in the values 0.091, 0.082, 0, and -0.063 for acetonitrile, methanol, ethanol, and propanol, respectively. Such  $N_+$  estimated values suggest very similar nucleophilicity among solvents.

Do solvent mixtures exhibit the same behavior? Minegishi et al. evaluated first-order kinetic constants of different benzhydrylium ions in binaries mixtures of water/alcohol and water/acetonitrile and also concluded that relative nucleophilicity of these solvents and mixtures are similar and fairly independent of carbocation electrophilicities.<sup>10</sup> Our kinetic data of aryldiazonium solvolysis in the solvent mixtures (not shown) also support similar nucleophilicities. Bravo-Diaz et al.<sup>9,18</sup> analyzed the decomposition of substituted aryldiazonium cations mixture of solvents, observed low selectivity, and argued that product ratios must reflect the local concentration around the aryldiazonium cation.

Is there a relationship between preferential solvation and product ratios? We calculated local concentration of the solvents around diazonium ion from MD simulations. The local solvent composition depended linearly on  $x_{\text{water}}$  for water/methanol binary mixtures, but varied nonlinearly for the other solvent mixtures. The O atom (or N) solvated the ipso carbon or surrounded the -N<sub>2</sub> group, and there was no preference to interact with any other groups of the diazonium ion (Figure 4).

Our classical simulations showed, assuming an equal probability of reaction, that the calculated local number of solvent molecules around the aryldiazonium cation can predict the product ratios, when preferential solvation shell on ipso carbon site is considered (Figures 1–3). In addition, our simulations have also considered two different atomic charge

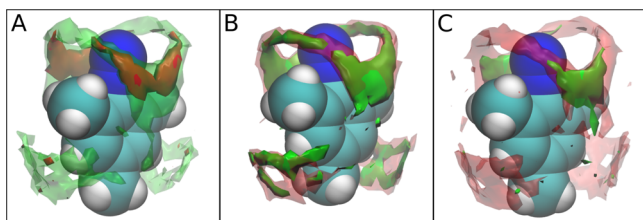


**Figure 4.** Spatial distribution of the oxygen atom of water (red surface) or methanol (green surface) in MD simulations with  $x_{\text{water}}$  equal to (A) 0.25; (B) 0.50; and (C) 0.75.

distributions, i.e., an atomic charge distribution considering electrons delocalized over all molecule (M2 model) and atomic charge distribution considering electrons delocalized over aryl cation and a neutral  $\text{N}_2$  moiety (M1 model). Such models changed the atomic charge on ipso carbon of  $-0.46|e|$  to  $+0.61|e|$  going from M2 to M1 model, respectively. As presented above (Figures 1–3), our product predictions were only slightly dependent on the ipso carbon atomic value.

The charge sign inversion on the ipso carbon is linked to the total dipole moment vector behavior: an inversion of its direction changes the atomic charge on the carbon site (Figure 5). Total electrostatic potential was also calculated at the

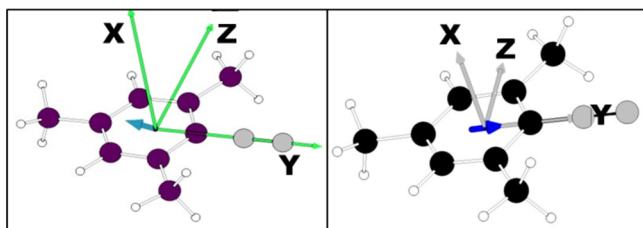


**Figure 5.** Dipole moments (blue arrows) of the aryl-diazonium cation in M1 (left) and M2 (right) charge models.

B3LYP/TZVPP level for both aryl-diazonium cation and a nonrelaxed aryl cation systems (Figure 6). Although the total electrostatic potentials are different on the center of ipso carbon nucleus, comparison between electrostatic potentials does not show significant deviation above 0.2 nm.

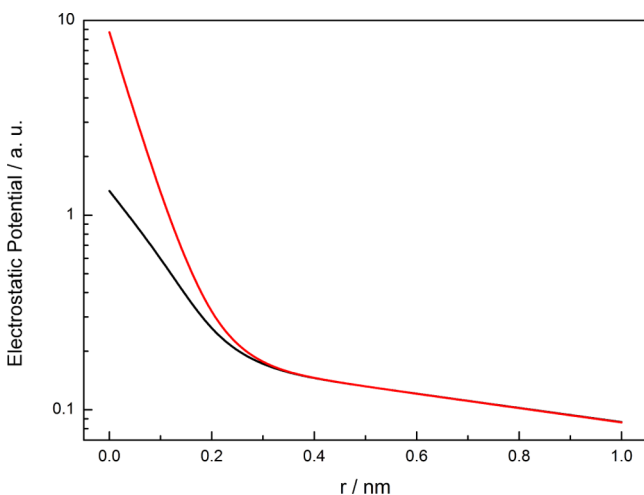


**Figure 6.** Total electrostatic potential at B3LYP/TZVPP level calculated on the ipso carbon site and above it. Black and red lines represent the aryl-diazonium cation and the phenyl cation, respectively.

Even though a product prediction ratio is possible, a molecular understanding of the complete process is still lacking. Probably, calculations of reactive trajectories (as in ref 13) will be necessary if we want to deeply understand the assumption of equal probabilities.

## EXPERIMENTAL SECTION

**Materials.** Methanol, ethanol, *n*-propanol, 2-propanol, and acetonitrile were HPLC grade, and 2,4,6-trimethylphenol (1-ArOH) and trimethylbenzene (1-ArH) were used as received. 2,4,6-trimethylbenzenediazonium (1-ArN<sub>2</sub><sup>+</sup>) tetrafluoroborate and 2,6-dimethyl-4-hexadecylbenzenediazonium tetrafluoroborate (16-ArN<sub>2</sub><sup>+</sup>) were synthesized as described.<sup>1,2</sup> The compounds 2,6-dimethyl-4-hexadecyl-aniline (used in the synthesis of 16-ArN<sub>2</sub><sup>+</sup>), 2,6-dimethyl-4-hexadecyl-phenol, 16-ArOH, and 2,6-dimethyl-4-hexadecyl-benzene (15-ArH) were kindly furnished by Dr. L. Romsted. 2,4,6-benzeneacetamide (1-ArNHAc) and 2,6-dimethyl-4-hexadecyl-benzeneacetamide, 16-ArNHAc, were synthesized as described.<sup>18,19</sup>

Synthesis of 2,4,6-trimethylanisole (1-ArOMe) and 2,6-dimethyl-4-hexadecylanisole (16-ArOMe): 500 mg of 1-ArN<sub>2</sub><sup>+</sup> or 16-ArN<sub>2</sub><sup>+</sup> were added to 100 mL of methanol containing 50  $\mu\text{L}$  of an aqueous solution of HCl 1.0 mol dm<sup>-3</sup> and maintained at 30 °C for 24 h. After solvent evaporation, water was added, and the product extracted with chloroform. Na<sub>2</sub>SO<sub>4</sub> was added to the chloroform to remove traces of water and filtered. Chloroform was evaporated, and the product was purified in a silica gel column G60 with CHCl<sub>3</sub>/hexane 75:25 (v/v).

The standard curves for the determination of the concentration of the compounds 2,4,6-trimethyl-1-ethoxy-benzene (1-ArOEt), 2,6-dimethyl-4-hexadecyl-1-ethoxybenzene (16-ArEt), 2,4,6-trimethyl-1-propoxy-benzene (1-ArOPr), and 2,6-dimethyl-4-hexadecyl-1-propoxybenzene (16-ArPr) were prepared from a solution of weighed 1-ArN<sub>2</sub><sup>+</sup> which was reacted in ethanol or propanol in the presence of 1.0  $\times 10^{-3}$  mol dm<sup>-3</sup> HCl. The percentage of 1-ArOH and 1-ArCl were <5% of the initial concentration of the diazonium salt.

## METHODS

**Product Analysis by HPLC.** Products of dediazonation reaction were analyzed in a HPLC equipped with a C-18 reverse phase column, using a loop of 30  $\mu\text{L}$ . Products were detected by absorption at 220 nm.

A solvent mixture of methanol/water 82:18 (v/v) was used to separate the products of dediazonation of 1-ArN<sub>2</sub><sup>+</sup> in the HPLC (retention times: 1-ArOH, 4.6 min; 1-ArOMe, 6.7 min; 1-ArOEt, 7.7 min; 1-ArOPr, 9.8 min; 1-ArH, 13.0 min) using a flux of 0.8 mL min<sup>-1</sup>. For experiments with acetonitrile/water mixtures, the solvent mixture used was methanol/water 75:25 (v/v), 0.8 mL min<sup>-1</sup> (retention times: 1-ArNHAc, 4.6 min; 1-ArOH, 6.8 min). The products 16-ArOH, 16-ArOMe, 16-ArOPr, and 16-ArNHAc were eluted with methanol/2-propanol 82:18 (v/v), with a flux of 1 mL min<sup>-1</sup> (retention times: 16-ArNHAc 5.1 min, 16-ArOH, 6.0 min, 16-ArOMe, 8.7 min, 16-ArOPr 9.2 min, and 16-ArH, 9.5 min).

The concentration of each product eluted in the HPLC was determined through a standard curve of area versus concentration obtained in the same HPLC conditions used for the samples. The percentage of products was calculated by dividing the concentration of each product by the sum of all products multiplied by 100.

**Dediazonation reaction of 1-ArN<sub>2</sub><sup>+</sup> and 16-ArN<sub>2</sub><sup>+</sup>.** All the solvents mixtures used in the dediazonation reactions contained HCl 0.001 or 0.002 mol dm<sup>-3</sup>, added from HCl 12.5 mol dm<sup>-3</sup> (ca. 0.010 mL per 100 mL of solvent). Pure solvents contained 0.55 mol dm<sup>-3</sup> of water due to the addition of HCl. All solvents mixtures used in the reactions were prepared by weight in 2 mL volumetric tubes.

Reactions were started by adding a small aliquot (0.025 or 0.030 mL) of a concentrated 1-ArN<sub>2</sub><sup>+</sup> solution (between 8 and 4  $\times 10^{-3}$  mol dm<sup>-3</sup>), diluted in the organic solvent, to the appropriate solvent mixture with a final volume of 1.0 mL in 2 mL tubes equipped with Teflon stoppers. The stock solutions of the diazonium salts were maintained in an ice-bath to avoid significant decomposition prior to

the addition to the solvent mixtures. A layer of 50  $\mu\text{L}$  of hexane was added over the reactions tubes with  $1\text{-ArN}_2^+$  to avoid products evaporation when the water content in the mixtures was higher than 80%. The addition of cyclohexane does not affect product distribution or solvent composition due to its low solubility in water.<sup>14</sup> After 24 h at 30  $^\circ\text{C}$ , the samples were diluted to 2 mL with *n*-propanol, to homogenize the solutions which were maintained at 8  $^\circ\text{C}$ , until HPLC analysis.

**Molecular Dynamics Simulations.** All simulations were performed with GROMACS 4.5.5 simulation package in double precision in a NPT ensemble.<sup>20</sup> The  $4 \times 4 \times 4$  nm edge initial box was built with Packmol package<sup>21</sup> and consisted of one  $1\text{-ArN}_2^+$  and different numbers of solvent molecules (water, methanol, ethanol, propanol, and acetonitrile), depending on the water molar fraction. A background negative charge is neutralizing the system. The number of solvent molecules was calculated from the molar fraction and the density of the systems.<sup>22–24</sup> The water model used was SPC/E, and the force field of the alcohols was OPLS-AA.<sup>25</sup> The force field for acetonitrile was taken from Wick et al.,<sup>26</sup> since it reproduces the amount of hydrogen-bonded acetonitrile molecules.<sup>27</sup> The equilibrium geometry of  $1\text{-ArN}_2^+$  was calculated with Gaussian 03 at B3LYP/6-31+G\* level.<sup>28–33</sup> Then, CHELPG<sup>34</sup> charges were calculated for the molecule with and without the  $-\text{N}_2$  group (nonrelaxed geometry), models M2 and M1, respectively, using ORCA v3.0.1 at B3LYP/TZVPP level using RIJCOSX technique in vacuum.<sup>35–38</sup> Note that in MD simulations with M1 model the nitrogen atoms have no partial charge (see Scheme S11 and Table S11). For modeling the intermolecular interactions, it is common practice to define and compute an atomic charge distribution representing the electrostatic potential around the molecule or their multipole moments. For such task, different protocols and ideas have been proposed, e.g., the RESP,<sup>39</sup> MK,<sup>40,41</sup> CHELP,<sup>42</sup> CHELPG,<sup>34</sup> CHELMO,<sup>43</sup> DDEC/cn,<sup>44</sup> CMx,<sup>45,46</sup> and multipole-derived charges.<sup>47</sup> In special case of an OPLS-consistent atomic charge model, Jorgensen et al. have suggested the CMx charge model and Canongia–Lopez et al. have used the CHELPG. Commonly, atomic charge models are based on RESP<sup>39</sup> or MK<sup>40,41</sup> protocol at HF/6-31G\* level in vacuum, but these were developed for aqueous systems, not mixtures. Alternatively, Jorgensen et al. have suggested the CMx charge model as an OPLS-consistent atomic charge model.<sup>48</sup> We are following Canongia–Lopez et al.<sup>49</sup> who have suggested the CHELPG protocol as a convenient way to generate an OPLS-consistent charge model. The charge distribution for M1 and M2 and other atomic parameters of  $1\text{-ArN}_2^+$  can be found in Supporting Information. All other  $1\text{-ArN}_2^+$  parameters were OPLS-AA.

The geometric combination rule was used for Lennard-Jones interactions. Coulomb forces were calculated using smooth particle-mesh Ewald summation with periodic boundary conditions. The cutoff radius of the Lennard-Jones interactions was equal to 1.2 nm, with a switching function starting at 1.1 nm. All simulations were performed at 303 K and 1 bar of pressure, maintained by isotropic pressure coupling using Parrinello–Rahman algorithm. Simulations were carried out for 20 ns, and the first 2 ns was not used for calculations.

The number of solvent molecules in the first solvation shell of the carbon in the aromatic ring (ipso) bound to the N atom was calculated as in eq 2:

$$N_Z = 4\pi\rho_Z \int_0^{r_1} g(r)r^2 dr \quad (2)$$

where Z refers to water, methanol, ethanol, propanol, or acetonitrile;  $\rho_Z$  is the density number of the molecule Z;  $g(r)$  is the radial distribution function between the atom ipso carbon and the oxygen atom of Z;  $r_1$  is the limit distance. Such distance is defined as the first minimum of  $g(r)$  or the first inflection point in the  $g(r)*r^2$  function.

The percentage of a Z nucleophile ( $\theta_Z$ ) around ipso carbon was defined as  $\theta_Z = 100N_Z/(N_Z + N_{Z'})$ , being Z' the other solvent in the simulated Z/Z' binary mixture.

## ■ ASSOCIATED CONTENT

### 📄 Supporting Information

The Supporting Information is available free of charge on the ACS Publications website at DOI: 10.1021/acs.joc.5b01289.

Arenediazonium cation structure and atomic charges; radial distribution function between ipso carbon and the oxygen atom of methanol and water in the methanol/water 50/50 simulation; description of the procedure to obtain the spatial distribution figures; mass spectra of the products (PDF)

Input files containing the force field parameters used in all simulations are available as well as the spatial configuration files for simulations with  $x_{\text{water}} = 50$  (ZIP)

## ■ AUTHOR INFORMATION

### Corresponding Authors

\*E-mail: filipe.lima@usp.br.

\*E-mail: imcuccov@iq.usp.br.

### Notes

The authors declare no competing financial interest.

## ■ ACKNOWLEDGMENTS

This work was partially financed by FAPESP Grant 2013/08166-5, a Post Doctoral Fellowship to F.S.L. (FAPESP, 2014/06073-2), CNPq for scholarships (to I.M.C. and H.C.), the Instituto Nacional de Ciência e Tecnologia de Fluidos Complexos (INCT-FCx, CNPq-FAPESP) and the Núcleo de Apoio à Pesquisa de Fluidos Complexos (NAP-FCx, USP). We acknowledge the Dr. Paolo Di Mascio for the use of the Mass Spectrometer and Dr. Fernanda Manso Prado, Luciana Coutinho de Oliveira, and Rafael Y. Vavrick for helpful discussions. We acknowledge also the Central Analítica do Instituto de Química da USP and MSc Janaina Vilcachagua and MSc Cristiane P. M. Xavier. We thank the anonymous referees for their careful revision and exceedingly helpful criticism of a previous version of this manuscript.

## ■ REFERENCES

- Jencks, W. P. *Catalysis in Chemistry and Enzymology*; McGraw-Hill: New York, 1987.
- Cuccovia, I.; Chaimovich, H. In *Catalysis and Photochemistry in Heterogeneous Media*; Brochsztain, I. L. N. a. S., Ed.; Research Signpost: 2007.
- Zollinger, H. *Diazo Chemistry I: Aromatic and Heteroaromatic Compounds*; Wiley-VCH: Weinheim, Germany, 1994; Vol 107, p 1917
- Wu, Z. Y.; Glaser, R. J. *Am. Chem. Soc.* **2004**, *126*, 10632.
- Cuccovia, I. M.; da Silva, M. A.; Ferraz, H. M. C.; Pliego, J. R.; Riveros, J. M.; Chaimovich, H. *J. Chem. Soc. Perkin Trans. 2* **2000**, 1896.
- Ussing, B. R.; Singleton, D. A. *J. Am. Chem. Soc.* **2005**, *127*, 2888.
- Martinez, A. G.; Cerero, S. D.; Barcina, J. O.; Jimenez, F. M.; Maroto, B. L. *Eur. J. Org. Chem.* **2013**, 2013, 6098.
- Fernandez-Alonso, A.; Bravo-Diaz, C. *J. Phys. Org. Chem.* **2010**, *23*, 938.
- Pazo-Llorente, R.; Bravo-Diaz, C.; Gonzalez-Romero, E. *Eur. J. Org. Chem.* **2004**, 2004, 3221.
- Minegishi, S.; Kobayashi, S.; Mayr, H. *J. Am. Chem. Soc.* **2004**, *126*, 5174.
- Bogle, X. S.; Singleton, D. A. *Org. Lett.* **2012**, *14*, 2528.
- Samanta, D.; Rana, A.; Schmittel, M. *J. Org. Chem.* **2014**, *79*, 2368.
- Thallmair, S.; Zaulck, J. P. P.; de Vivie-Riedle, R. *J. Chem. Theory Comput.* **2015**, *11*, 1987.

- (14) Chaudhuri, A.; Loughlin, J. A.; Romsted, L. S.; Yao, J. *J. Am. Chem. Soc.* **1993**, *115*, 8351.
- (15) Pastoriza-Gallego, M. J.; Bravo-Diaz, C.; Gonzalez-Romero, E. *Langmuir* **2005**, *21*, 2675.
- (16) Ritchie, C. D. *Acc. Chem. Res.* **1972**, *5*, 348.
- (17) Ritchie, C. D. *Can. J. Chem.* **1986**, *64*, 2239.
- (18) Pazo-Llorente, R.; Bravo-Diaz, C.; Gonzalez-Romero, E. *Langmuir* **2003**, *19*, 9142.
- (19) Romsted, L. S.; Yao, J. H. *Langmuir* **1996**, *12*, 2425.
- (20) Hess, B.; Kutzner, C.; van der Spoel, D.; Lindahl, E. *J. Chem. Theory Comput.* **2008**, *4*, 435.
- (21) Martinez, L.; Andrade, R.; Birgin, E. G.; Martinez, J. M. *J. Comput. Chem.* **2009**, *30*, 2157.
- (22) Gonzalez, B.; Calvar, N.; Gomez, E.; Dominguez, A. *J. Chem. Thermodyn.* **2007**, *39*, 1578.
- (23) Mikhail, S. Z.; Kimel, W. R. *J. Chem. Eng. Data* **1963**, *8*, 323.
- (24) Tamura, K.; Nakamura, M.; Murakami, S. *J. Solution Chem.* **1997**, *26*, 1199.
- (25) Jorgensen, W. L.; Maxwell, D. S.; TiradoRives, J. *J. Am. Chem. Soc.* **1996**, *118*, 11225.
- (26) Wick, C. D.; Stubbs, J. M.; Rai, N.; Siepmann, J. I. *J. Phys. Chem. B* **2005**, *109*, 18974.
- (27) Mountain, R. D. *J. Phys. Chem. B* **2010**, *114*, 16460.
- (28) Frisch, M. J.; Trucks, G. W.; Schlegel, H. B.; Scuseria, G. E.; Robb, M. A.; Cheeseman, J. R.; Montgomery, J. A., Jr.; Vreven, T.; Kudin, K. N.; Burant, J. C.; Millam, J. M.; Iyengar, S. S.; Tomasi, J.; Barone, V.; Mennucci, B.; Cossi, M.; Scalmani, G.; Rega, N.; Petersson, G. A.; Nakatsuji, H.; Hada, M.; Ehara, M.; Toyota, K.; Fukuda, R.; Hasegawa, J.; Ishida, M.; Nakajima, T.; Honda, Y.; Kitao, O.; Nakai, H.; Klene, M.; Li, X.; Knox, J. E.; Hratchian, H. P.; Cross, J. B.; Bakken, V.; Adamo, C.; Jaramillo, J.; Gomperts, R.; Stratmann, R. E.; Yazyev, O.; Austin, A. J.; Cammi, R.; Pomelli, C.; Ochterski, J. W.; Ayala, P. Y.; Morokuma, K.; Voth, G. A.; Salvador, P.; Dannenberg, J. J.; Zakrzewski, V. G.; Dapprich, S.; Daniels, A. D.; Strain, M. C.; Farkas, O.; Malick, D. K.; Rabuck, A. D.; Raghavachari, K.; Foresman, J. B.; Ortiz, J. V.; Cui, Q.; Baboul, A. G.; Clifford, S.; Cioslowski, J.; Stefanov, B. B.; Liu, G.; Liashenko, A.; Piskorz, P.; Komaromi, I.; Martin, R. L.; Fox, D. J.; Keith, T.; M. A. Al-Laham, Peng, C. Y.; Nanayakkara, A.; Challacombe, M.; Gill, P. M. W.; Johnson, B.; Chen, W.; Wong, M. W.; Gonzalez, C.; Pople, J. A. *Gaussian 03*; Gaussian, Inc.: Wallingford, CT, 2004.
- (29) Becke, A. D. *J. Chem. Phys.* **1993**, *98*, 5648.
- (30) Lee, C.; Yang, W.; Parr, R. G. *Phys. Rev. B: Condens. Matter Mater. Phys.* **1988**, *37*, 785.
- (31) Vosko, S. H.; Wilk, L.; Nusair, M. *Can. J. Phys.* **1980**, *58*, 1200.
- (32) Stephens, P. J.; Devlin, F. J.; Chabalowski, C. F.; Frisch, M. J. *J. Phys. Chem.* **1994**, *98*, 11623.
- (33) Ditchfield, R.; Hehre, W. J.; Pople, J. A. *J. Chem. Phys.* **1971**, *54*, 724.
- (34) Breneman, C. M.; Wiberg, K. B. *J. Comput. Chem.* **1990**, *11*, 361.
- (35) Neese, F. *Wiley Interdisciplinary Reviews: Computational Molecular Science* **2012**, *2*, 73.
- (36) Schafer, A.; Horn, H.; Ahlrichs, R. *J. Chem. Phys.* **1992**, *97*, 2571.
- (37) Weigend, F.; Ahlrichs, R. *Phys. Chem. Chem. Phys.* **2005**, *7*, 3297.
- (38) Kossmann, S.; Neese, F. *Chem. Phys. Lett.* **2009**, *481*, 240.
- (39) Bayly, C. I.; Cieplak, P.; Cornell, W. D.; Kollman, P. A. *J. Phys. Chem.* **1993**, *97*, 10269.
- (40) Besler, B. H.; Merz, K. M.; Kollman, P. A. *J. Comput. Chem.* **1990**, *11*, 431.
- (41) Singh, U. C.; Kollman, P. A. *J. Comput. Chem.* **1984**, *5*, 129.
- (42) Chirlian, L. E.; Francl, M. M. *J. Comput. Chem.* **1987**, *8*, 894.
- (43) Sigfridsson, E.; Ryde, U. *J. Comput. Chem.* **1998**, *19*, 377.
- (44) Manz, T. A.; Sholl, D. S. *J. Chem. Theory Comput.* **2012**, *8*, 2844.
- (45) Thompson, J. D.; Cramer, C. J.; Truhlar, D. G. *J. Comput. Chem.* **2003**, *24*, 1291.
- (46) Marenich, A. V.; Jerome, S. V.; Cramer, C. J.; Truhlar, D. G. *J. Chem. Theory Comput.* **2012**, *8*, 527.
- (47) Simmonett, A. C.; Gilbert, A. T. B.; Gill, P. M. W. *Mol. Phys.* **2005**, *103*, 2789.
- (48) Udier-Blagovic, M.; De Tirado, P. M.; Pearlman, S. A.; Jorgensen, W. L. *J. Comput. Chem.* **2004**, *25*, 1322.
- (49) Lopes, J. N. C.; Deschamps, J.; Padua, A. A. H. *J. Phys. Chem. B* **2004**, *108*, 2038.